# ADVANCES IN THE BONDLINE CONTROL TECHNOLOGY FOR THE CERTIFICATION OF ADHESIVELY BONDED COMPOSITE REPAIRS

Lennert Heilmann[1], Peter Wierach[2] and Martin Wiedemann[3]

German Aerospace Centre (DLR e.V.),
Institute of Composite Structures and Adaptive Systems,
Lilienthalplatz 7, 38108 Brunswick, Germany
www.dlr.de
[1] lennert.heilmann@dlr.de,
[2] peter.wierach@dlr.de
[3] martin.wiedemann@dlr.de

**Keywords:** Composite repair, Adhesive bonding, Weak bond detection, Contaminants

## ABSTRACT

Adhesively bonded composite repairs restoring limit load capacity are not yet certified in civil aviation due to a lack of methods suitable for the substantiation of proper bond quality. In our previous paper, we proposed a novel method for process control to resolve this issue [1]. The core of this bondline control technology is a new type of adhesion test that provides proof of bond quality and simultaneously serves as a robust surface pre-treatment for adhesive bonding.

The present study describes improvements implemented in the adhesion test and demonstrates the ability of the test to detect bonding defects. Furthermore, the applicability on stepped surfaces common for repair scenarios is investigated. Finally, a test series on the quality of the surface pre-treatment is presented.

## 1 INTRODUCTION

The use of fibre-reinforced plastics (FRPs) in primary structures of large civil aircraft is steadily increasing, yet the repair of such structures continues to pose a particular challenge [2, 3]. Currently, only bolted joints are certified for safety-critical repairs in passenger aircraft, but this technology is rather disadvantageous when applied to FRPs. In particular, the drilling of bolt holes leads to a severe reduction in structural strength, which is why FRP components must sometimes be manufactured with considerable material allowances for the possible event of such a repair [2].

Adhesive bonding is a very efficient technology for the repair of FRPs, but is currently limited to non-critical joints. This is due to the regulations of the civil aviation authorities, which demand proof that proper bond strength has been achieved in safety-critical repairs [4, 5, 6]. Until today no feasible inspection method is available that can provide this proof of bond strength [2, 3].

The necessity for such rigorous conservatism becomes especially apparent in the case of adhesively bonded repairs, since the bondability of a FRP structure that has been in operation cannot be verified in generic materials and process qualifications. This is due to the fact that at the time of the occurrence of the damage, the part has had an individual history in which it was exposed to the in-service environment. The entirety of in-service related influences that may have a negative impact on an adhesive bond to be produced cannot be reproduced for qualifications in a lab. Thus, a comprehensive bondability envelope cannot be defined for the repair process.

## 2 THE BONDLINE CONTROL TECHNOLOGY

In order to achieve the means of compliance for the certification of adhesively bonded repairs in structural applications, a novel method has been invented (patent pending) that was originally presented in our previous article [1]. The core of this bondline control technology is to perform an adhesion test on the entire joining surface prior to the application of the repair patch. The mechanical

test serves as proof that proper bond quality has been achieved between the adhesive and the individual FRP structure. By means of a sufficiently high sensitivity of the test it must be ensured that all technically relevant defects present in the bondline are detected by the fracture pattern or as a deviation from the target failure load. A technically relevant defect is defined as a deviation from the nominal condition of the bond which can lead to damage to the joint within the intended operating life of the component and within the framework of the operating conditions and events to be taken into account in the design. The technical relevance of a defect thus depends on the respective application.

The use of qualified materials, qualified material combinations and the application of qualified manufacturing processes must ensure that a subsequent degradation of a non-defective bond is excluded under the permissible operating conditions. Any defects are assumed to origin in the production of the bond and are therefore already present at the time of completion of the joint as a deviation from the target condition. Under this premise, an inspection directly after production is sufficient to guarantee the required quality of the bonded joint throughout the operational life.

In case that adequate bond quality is confirmed by the test, a thin layer of well-attached adhesive with an optimised surface remains in the patch application area that acts as a bonding primer. In a subsequent step, the repair patch is bonded onto this layer of tested adhesive. Since the tested adhesive consists of fresh material and its surface is generated reproducibly, it features a defined bondability. Therefore, a process envelope can be developed via a materials and process qualification that ensures proper quality of the bond produced on this surface. In addition to checking the bonded patch with conventional inspection techniques, mechanical test coupons can be installed adjacent to the patch on surplus tested adhesive. Since the tested adhesive surface exhibits homogeneous bonding properties, the test results obtained from these specimens can be considered representative for the entire bonded repair patch. Thus, final proof of the quality of the adhesive bond is provided. For an illustrated description of the novel proof concept, the reader is kindly referred to our previous article [1].

Our approach is to realise the adhesion test by bonding a porous fabric (see Fig. 1) onto the patch application area and subsequently peeling it. Due to the mechanical interlocking of the fabric and the adhesive, a high mechanical stress is generated in the bondline during peeling, which leads cohesion failure of the adhesive. This way, a surface pre-treatment of the tested adhesive is achieved simultaneously. The peeling of porous fabrics result in a very defined layer of adhesive with an optimised surface that is especially well-suited for the formation of a strong and durable bond. It is claimed that bonding on this type of surface can be done with the same process reliability as in wet-wet interface bonding.

## 3 PREVIOUS AND CURRENT RESEARCH

In our previous paper, we described the screening process for suitable peeling materials that led to the selection of square mesh fabrics (SMFs). In order to characterise the mechanical behaviour of these fabrics in the peeling process, a new type of test coupon was defined. A series of these coupons manufactured with different SMFs was tested with the floating roller peel method according to EN 2243-2 [7]. The test series showed that a defined load can be introduced into the bondline by means of porous fabrics and that the load can be widely adjusted by means of different fabric parameters. The analysis also showed that peeling these fabrics produces a surface that is highly textured and mainly fractured cohesively.

In the current study, advances in the development of the novel bondline control technology are presented. Dutch weave fabrics are introduced as a new type of test fabric that enable the manufacturing of an improved version of the test coupon. An example case is made with specimens featuring artificial defects to demonstrate the capability of the peel test to detect bonding defects via the fracture pattern and via the peeling diagram. The ability of the test method to be applied on realistic repair surface geometries is evaluated by tests performed on stepped carbon fibre reinforced plastic (CFRP) panels. The experimental part ends with an assessment of the bondability of the fractured layer of adhesive that is produced by peeling of porous fabrics embedded in epoxy. This study is carried out via double cantilever beam (DCB) specimens.

## 4 EXPERIMENTS

In the following sections, the materials and processes used in our experiments, improvements in the practical implementation of our method and the test series and results are presented.

### 4.1 Materials and processes

All adhesion tests were performed on pre-cured carbon fibre reinforced plastics with an epoxy matrix as described in Table 1. The surface activation of the laminates prior to bonding was realised by wet grinding with aluminium oxide sand paper under de-ionised water. The adhesive used is a 1C-epoxy adhesive film with a nominal thickness of 0,25 mm and a non-woven polyester carrier material. The adhesive is denoted as *adhesive A* in the further course of this paper. Curing of the adhesive was performed at 120 °C in a circulating air oven under vacuum according to the manufacturer's instructions.

| Substrate code | Type of material | Representation |
|---|---|---|
| *CFRP A* | Unidirectional prepreg tape | Original airframe material |
| *CFRP B* | Unidirectional prepreg tape | Out of autoclave repair material |
| *CFRP C* | Fabric prepreg | Generic substrate |

Table 1: CFRP materials used in the experiments.

The peel specimens were manufactured in the style of the floating roller peel test with a bonded width of 25 mm and an evaluated peeling length of 150 mm. Specimens manufactured with square mesh fabrics (SMFs) were designed with a sealed edge as described in our previous paper [1]. Testing of the peel specimens was performed with an electromechanical testing machine *Zwick 1464* and a load cell *Zwick/Roell Xforce HP* with a nominal force of 2,5 kN. A test fixture according to EN 2243-2 [7] was used and the rate of peeling was set to 100 mm/min. All tests were performed at room temperature and the specimens were not conditioned.

### 4.2 New fabric and improved coupon geometry

In our previous research we found that square mesh fabrics (SMFs) made from polyester are a suitable means of introducing a high load into a thin bondline. However, the tests have also shown that SMFs have certain properties that complicate their application in the novel test method. Most importantly, the open weave style can in some cases require edge sealing of the fabric to prevent it from ripping during the peel test. In our recent research, dutch weave fabrics (DWFs) were identified as an alternative type of porous fabric that can be used to perform the adhesion test. Fig. 1 shows a scanning electron microscope (SEM) image of a SMF and of a DWF for comparison of the different weave styles.

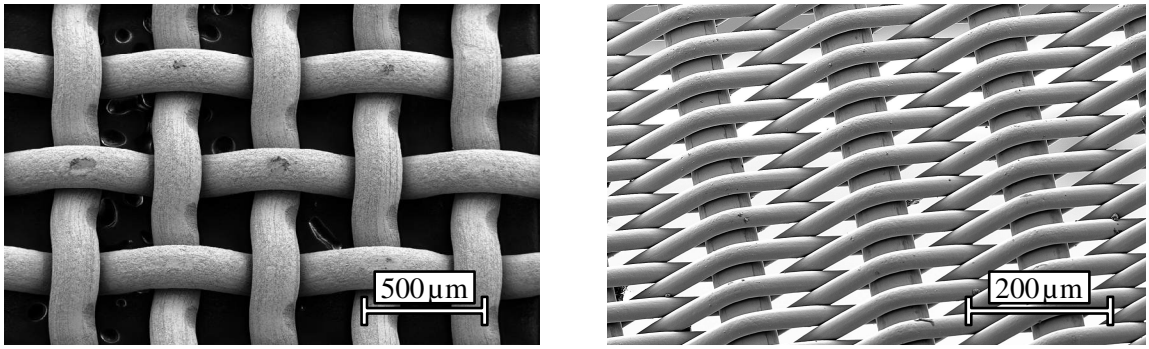


Figure 1: SEM images of fabric types proposed for the adhesion test. Left: a SMF. Right: a DWF.

It was found that DWFs possess certain advantages over SMFs. Most importantly, DWFs feature a higher mechanical strength and stability than SMFs and therefore can be peeled in any fabric orientation angle without ripping at trimmed edges. This specific property allows the manufacturing of an improved test coupon that does not require edge sealing (patent pending). This improved coupon is depicted in Fig. 2 in the peeled and in the unpeeled state. The tested DWFs have a pore size of less than 50 µm, which results in a fracture surface with a very homogeneous appearance that greatly improves the ability to visually identify bonding defects.

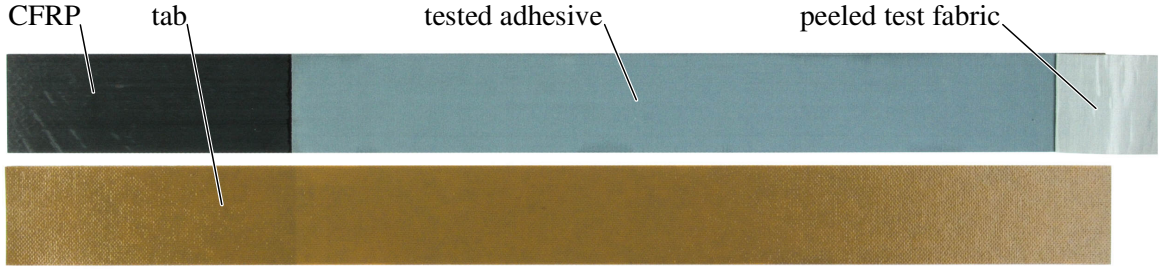


Figure 2: Improved test coupon without edge sealing. Bottom: unpeeled state. Top: peeled state.

### 4.3 Detection of defects: principle capability

In order to demonstrate the capability of the method to indicate bonding defects via the fracture pattern and via the peeling diagram, specimens were manufactured with artificial defects. A panel of pre-treated *CFRP C* was contaminated with a paint marker and subsequently a polyester SMF was bonded onto the substrate with *adhesive A*. The test area of each specimen was contaminated with 12 painted circles, starting with a diameter of 1 mm. The diameter of the following circles was increased in increments of 1 mm. After bonding, peel specimens with sealed edges were extracted from the panel.

Fig. 3 shows the test result of one of the contaminated specimens. On the lower part of Fig. 3 the substrate with the tested bond as well as the underside of the fully peeled fabric are shown. All 12 circles can be identified in the test area and on the peeled fabric, which indicates that cohesion failure occurred within the paint. The upper part of Fig. 3 shows the peeling diagram of the specimen. While the load reaches the reference value in the uncontaminated areas, each circle of paint can be allocated to a drop in the peeling force. The width and the magnitude of the drop in load correlates to the size of the respective paint circle.

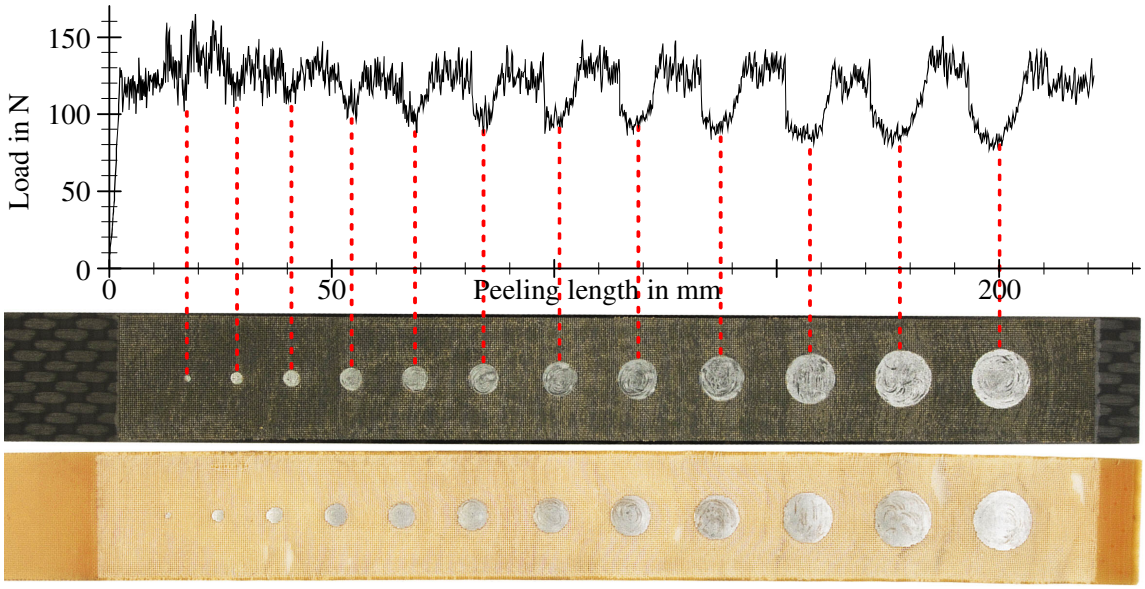


Figure 3: Test result of a defective bond. Bottom: peeled specimen and fabric. Top: peeling diagram.

The working principle of the peel test is similar to that of a line-scan. It is assumed that at any point during the peeling process, the load is distributed along a line that is oriented in the width direction of the specimen. The lateral extension of the loaded part of the bond comprises only one or a few rows of adhesive grid points that are interlocked in the pores of the fabric. During the test, the loaded line propagates in the direction of peeling. The load at one point of the peeling diagram is recorded when a row of adhesive grid points is fractured. Subsequently, the next row is loaded until fracture. This way, the continuous curve is generated. The singular load value measured at one point of the peeling diagram represents the average resistance of the bond along the loaded line at the corresponding section of the specimen. If the resistance of the bond is inhomogeneous along the loaded line, then the measured load is comprised of different fractions with different individual resistances.

As a result, the detectability of a defect as a drop or peak of load in the peeling diagram is dependent on its fraction of the width of the bonded area and its relative deviation from the resistance of a non-defective bond. A defect that extends in the width direction of the specimen is easier to detect in the peeling diagram than a defect oriented in the direction of peeling. And for a defect of a fixed size, the detectability via the peeling diagram is improved by decreasing the width of the peeled fabric.

Similarly, calculating the average peel force or average peel resistance over large peeling lengths reduces the relative impact of a defect on the resultant singular value. If defects must be detected automatically by means of an evaluation of the peel force, the width of the fabric strips as well as the length of the evaluated peeling length need to be defined according to the maximum allowable defect.

The threshold for the visual detection of bonding defects was found to be very low. Due to the homogeneity of the fractured surface (see Fig. 2) and the high resolution of the human eye, even minute defects of the size of a few fabric pores can be clearly identified.

### 4.4 Testing on stepped surfaces

In order to assess the applicability of the adhesion test on repair surface geometries, test coupons were produced with stepped CFRP panels. The panels consisted of the unidirectional tape material *CFRP A* in a quasi-isotropic layup and the surface comprised 8 plies forming 7 straight steps of 12 mm width and 0,18 mm depth each. A SMF and a DWF were bonded onto the panels via *adhesive A*. For both types of fabric, the test was carried out with the peeling direction down the steps, up the steps and along the steps. Those specimens featuring a peeling direction along the steps were manufactured with a width of 50 mm, all other specimens had the standard width of 25 mm.

The result of this series of tests was that independent of the type of fabric and independent of the peeling direction, no substrate damage occurred at the edges of the steps. Fig. 4 shows a peeled specimen representative of the test series. The pictured specimen was produced with a DWF and was peeled along the steps.

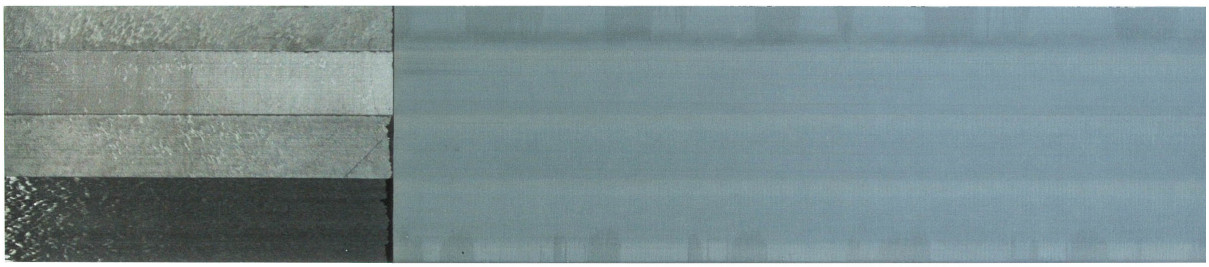

Figure 4: Fracture surface of a peel test performed alongside the steps of a stepped panel.

The peeling diagrams recorded showed uniform load curves with no significant disturbances. In case of the specimens peeled up and down the steps, some minor drops in peel force were observed when peeling over the edges of the steps. These drops in force accounted for around 3-5 % of the average load. For all specimens, the average peeling resistance was identical to reference values originating from specimens with flat surfaces.

### 4.5 Bondability of the fractured surface

One of the key features of the novel adhesion test is the ability to reproducibly generate a thin layer of tested adhesive with a fractured surface that is suitable for the formation of a strong and durable bond without further surface treatment. The thickness of the tested layer of adhesive and the morphology of the fractured surface are highly dependent on the type of fabric used and the interaction between the adhesive and the surface of the fabric filaments. In our experiments we found that with standard specifications of the presented fabric types, very thin layers of tested adhesive can be produced which result in a marginal increase of the overall bond thickness after a subsequent joining process with a film adhesive. Fig. 5 shows the process of peeling a DWF from a CFRP substrate and the tested adhesive layer that remains on the component. In this case, the tested adhesive has a peak thickness of around 65 µm and a levelled thickness of around 30 µm. With other fabric specifications, adhesive layers with levelled thicknesses of as little as 10 µm can be produced.

In Fig. 6, two scanning electron microscope (SEM) images of fractured surfaces with different morphologies are presented. The left image shows the surface generated by peeling of a SMF and the right image shows the surface generated by peeling of a DWF.

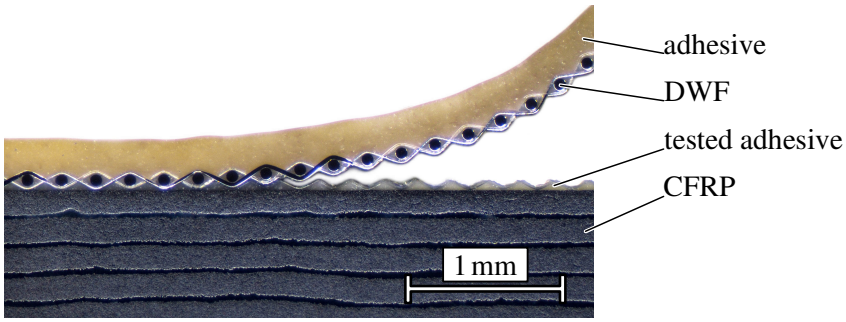


Figure 5: Microscopic image of the peeling process of a DWF (cross-sectional view).

By means of the DCB test, we evaluated the bondability of the fracture surfaces produced by different types of test fabrics. To manufacture the DCB specimens, substrate panels made from *CFRP A* were sanded and subsequently the respective test fabrics were bonded onto the substrate surface via *adhesive A*. After curing, the fabrics were peeled and a second adherend was adhesively bonded onto the fractured surface to produce the specimen panel. Table 2 shows the different configurations assessed in the test series. The fabrics used resulted in fractures with smooth fibre imprint surfaces as shown in Fig. 6. $\bar{A}_c$ is the percentage of the projected surface area that is fractured cohesively after peeling the respective fabric.

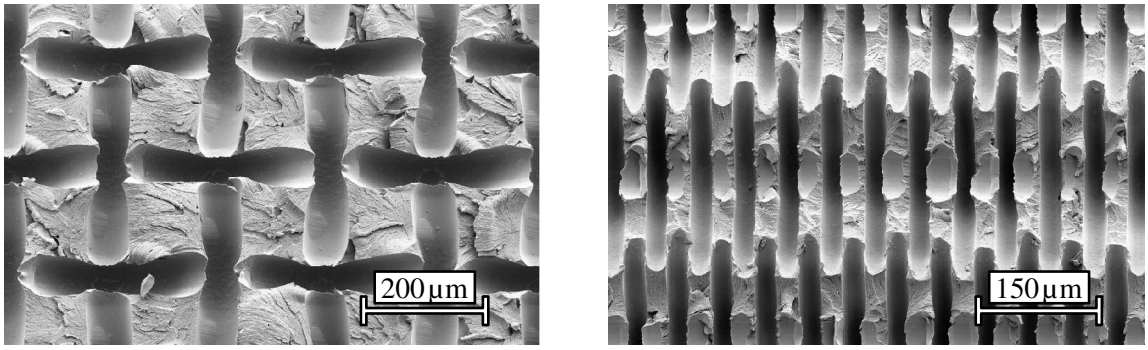


Figure 6: SEM images of fractured adhesive surfaces. Left: a surface generated with a SMF. Right: a surface generated with a DWF.

Configuration *DCB A* was produced by laminating fresh prepreg of *CFRP B* directly onto the tested adhesive layer generated by peeling a DWF made of stainless steel. Thus, the adhesive joint was formed by the epoxy resin of the prepreg without the use of a second adhesive film. The result is a

joint consisting of a very thin bondline without any carrier material inside the adhesive. A cross-sectional image of the bondline produced is shown in Fig. 7. Reference specimens were produced in a standard co-bonding process by bonding *CFRP B* prepreg onto a sanded panel of *CFRP A* with an intermediate layer of *adhesive A*.

| Configuration | Joining method | Test fabric | $\bar{A}_c$ | Test fabric material |
|---|---|---|---|---|
| *DCB A* | Co-bonding | DWF | 32 % | Stainless steel, untreated |
| *DCB B* | Secondary bonding | DWF | 32 % | Stainless steel, untreated |
| *DCB C* | Secondary bonding | SMF | 49 % | Stainless steel, untreated |
| *DCB D* | Secondary bonding | SMF | 47 % | Polyester, medical grade cleaned |
| *DCB E* | Secondary bonding | SMF | 40 % | Polyester, untreated |

Table 2: Configurations of DCB specimens produced via the novel method.

The specimen configurations *DCB B* to *DCB E* were made by bonding a second panel of pre-cured *CFRP A* onto the tested adhesive by means of *adhesive A*. This results in a bondline consisting of two layers of adhesive as illustrated in Fig. 8. Reference specimens were produced in a standard secondary bonding process by bonding two pre-cured panels of *CFRP A* via a layer of *adhesive A*.

Each test set consisted of six specimens. All configurations were tested in dry condition and most configurations were additionally tested in wet condition. The wet specimens were conditioned in a constant climate chamber at 80 °C and 85 % relative humidity for eight months to reach full saturation in accordance with DIN EN 2823 [8]. Testing was performed at room temperature (RT). The different types of failure modes distinguished as well as the abbreviations used are listed in Table 3. The area proportion of the different failure modes was analysed in the machine-tested *evaluation region A* of the specimens (see Fig. 10) by means of a digital imaging software.

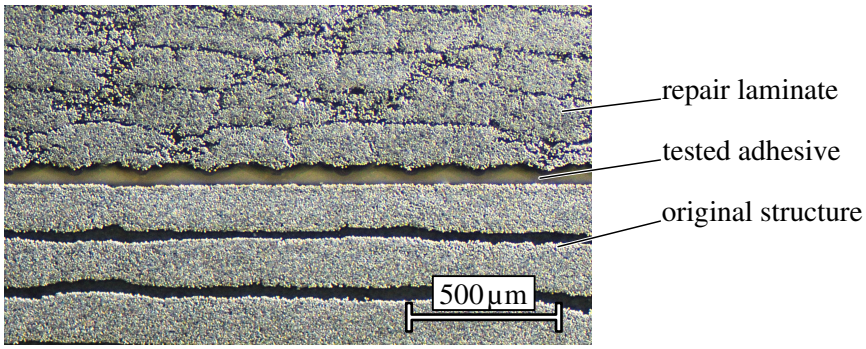


Figure 7: Microscopic image of the specimen configuration *DCB A* (cross-sectional view).

Table 4 shows the test results of the co-bonded specimen configuration *DCB A* and the corresponding reference. The fracture toughness is given relative to the reference value in dry condition, *v* indicates the coefficient of variation of the fracture toughness. The dominant failure mode of the co-bonded specimens was substrate failure (SF) inside the co-bonded laminate. The reference specimens showed some cohesion failure (CF), while the configuration *DCB A* showed substrate failure only. For all configurations, no adhesion failure (AF) and no special adhesion failure (SAF) could be identified. For both, the reference and configuration *DCB A*, a higher $G_{IC}$ value was measured for the wet specimens than for the dry specimens. It is assumed that the reason behind this is the plasticising effect that moisture can have on certain epoxies, as has already been found in other research [9]. In comparison to the reference, the specimens of configuration *DCB A* showed a lower $G_{IC}$ value. The reason behind this is that for the material combination tested, cohesion failure of the adhesive leads to higher $G_{IC}$ values than a crack propagating in either of the laminates. The *DCB A* specimens showed pure substrate failure, while the reference specimens had a portion of cohesion failure, which therefore resulted in a higher overall $G_{IC}$ value for the reference.

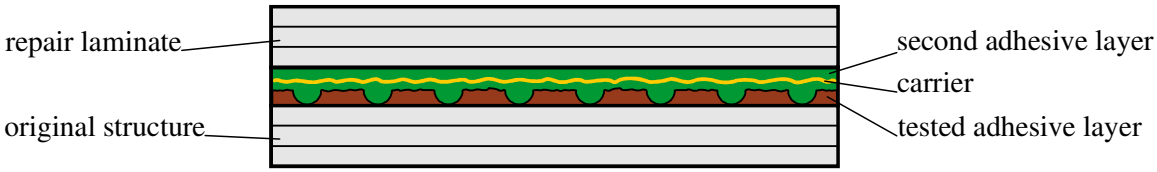


Figure 8: Illustration of a bondline consisting of two layers of adhesive (cross-sectional view).

One of several reasons why no crack propagation occurred inside the adhesive for *DCB A* specimens is assumed to be the absence of the carrier material in the bondline. While the carrier material acts as a crack stopper leading to high $G_{IC}$ values, it also functions as a crack attractor due to low adhesion between the adhesive and the carrier filaments. Since the carrier was fully removed during the production of the *DCB A* specimens, the crack propagation path led through the laminate. However, no adhesion failure occurred and mode I peeling is a load case not dominant in properly designed joints of a structure. Therefore, the test shows that an adhesive bond of high quality can be formed by directly laminating onto the fractured surface produced by peeling the test fabric.

Table 5 shows the test results of the secondary bonded specimen configurations. The dominant failure mode of all secondary bonded specimens was cohesion failure, accompanied by some substrate failure and minor porosity. For the specimens featuring two layers of adhesive, the substrate failure took place only in the repair laminate, which indicates that the substrate representing the original structure was not damaged by peeling the test fabrics.

| Abbreviation | Failure location |
|---|---|
| CF | Cohesion failure inside the adhesive |
| SF | Substrate failure of either of the substrate materials |
| AF | Adhesion failure at the interface between the adhesive and either of the substrates |
| SAF | Adhesion failure at the interface of the fractured adhesive layer |
| PO | Porosity inside the adhesive |

Table 3: Abbreviation and definition of the failure loci of the DCB specimens.

None of the specimens showed adhesion failure (AF). However, the specimens prepared with the polyester fabric showed some special adhesion failure (SAF) at the interface of the two layers of adhesive. Fig. 9 shows the image of an area with a spot of special adhesion failure. The adhesion failure occurred only on the fibre imprint surfaces and not on the square areas resulting from the fabric pores. It can be seen that cohesion failure took place in the square areas and that some carrier material is left on the squares that were originally free of carrier material after the peeling of the test fabric. The percentage of special adhesion failure given in Table 5 accounts for the total area affected by SAF, including cohesive squares surrounded by the adhesion failure at the fibre imprints.

| Configuration | Test condition | $G_{IC}$ | $v$ | CF | SF | AF | SAF | PO |
|---|---|---|---|---|---|---|---|---|
| *Ref.* | RT, dry | 100 % | 45,7 % | 29 % | 71 % | 0 % | 0 % | 0 % |
| *Ref.* | RT, wet | 107 % | 4,8 % | 25 % | 75 % | 0 % | 0 % | 0 % |
| *DCB A* | RT, dry | 50 % | 8,6 % | 0 % | 100 % | 0 % | 0 % | 0 % |
| *DCB A* | RT, wet | 60 % | 5,7 % | 0 % | 100 % | 0 % | 0 % | 0 % |

Table 4: Test results of configuration *DCB A* and the corresponding reference.

In their paper about the bondability of fracture surfaces generated with different peel plies, *L.-J. Hart-Smith et al.* note that even clean polyester filaments leave behind an inert surface that is not bondable by every type of adhesive [10]. Our experiments support these findings, since medical grade cleaned polyester was used in configuration *DCB D* and no residues could be found on the surface with the aid of a SEM. The inertness of the epoxy surface can be attributed to an interaction between

the molecules of the nonpolar thermoplastic surface and the monomers of the epoxy adhesive during the curing process. According to the findings of [11, 12], the polar functional groups of an uncured adhesive orient themselves away from the interface when in contact with a material that has a low surface energy. In contrast, a material with a high surface energy attracts the polar functional groups of the adhesive.

Due to the high surface energy of the metallic fabric filaments used in our experiments, the polar functional groups of the epoxy adhesive orient themselves towards the interface during the curing process. The subsequent peeling of the metal fabric exposes smooth fibre imprint surfaces that are wettable and highly reactive. This fundamental principle is validated by the presented test results, which show that the interface between the two layers of adhesive features an exceptional quality in case of the specimens produced with steel fabrics, resulting in no single occurrence of adhesion failure at the interface with the fibre imprint surface. The resulting fracture pattern is demonstrated by two tested specimens of configuration *DCB C*, shown in Fig. 10.

| Config. | Test condition | $G_{IC}$ | *v* | CF | SF | AF | SAF | PO |
|---|---|---|---|---|---|---|---|---|
| *Ref.* | RT, dry | 100 % | 10,2 % | 60,0 % | 39,5 % | 0 % | 0 % | 0,5 % |
| *DCB B* | RT, dry | 113 % | 18,1 % | 75,5 % | 21,5 % | 0 % | 0 % | 3,0 % |
| *DCB B* | RT, wet | 76 % | 5,9 % | 91,5 % | 6,5 % | 0 % | 0 % | 2,0 % |
| *DCB C* | RT, dry | 137 % | 13,9 % | 89,5 % | 7,5 % | 0 % | 0 % | 3,0 % |
| *DCB C* | RT, wet | 80 % | 5,5 % | 91,0 % | 7,5 % | 0 % | 0 % | 1,5 % |
| *DCB D* | RT, dry | 142 % | 20,0 % | 75,5 % | 14,0 % | 0 % | 10,0 % | 0 % |
| *DCB D* | RT, wet | 88 % | 5,9 % | 79,0 % | 6,5 % | 0 % | 12,5 % | 2,0 % |
| *DCB E* | RT, dry | 120 % | 14,2 % | 51,5 % | 3,5 % | 0 % | 45,0 % | 0 % |

Table 5: Test results of secondary bonded DCB specimen configurations.

The specimens depicted in Fig. 10 show a darker and a lighter side of the fractured bondline. The reason for this effect is that the crack propagation took place along the carrier material of the second adhesive film, which is positioned off-center in the bondline (see Fig. 8). This results in a thicker layer of adhesive remaining on one side than on the other, which then leads to the perception of a different colour and brightness of the adhesive. As explained before, the carrier material acts as a crack attractor. This proposition is supported by the results of the presented test series, since cohesion failure occurred along the carrier material of the second layer of adhesive for all specimens.

As for the fracture toughness values recorded, the reference shows a lower $G_{IC}$ value than the other secondary bonded configurations tested in dry condition. This can be explained by the higher portion of substrate failure that occurred in the reference and the lower general fracture toughness of the substrate material in comparison to the adhesive.

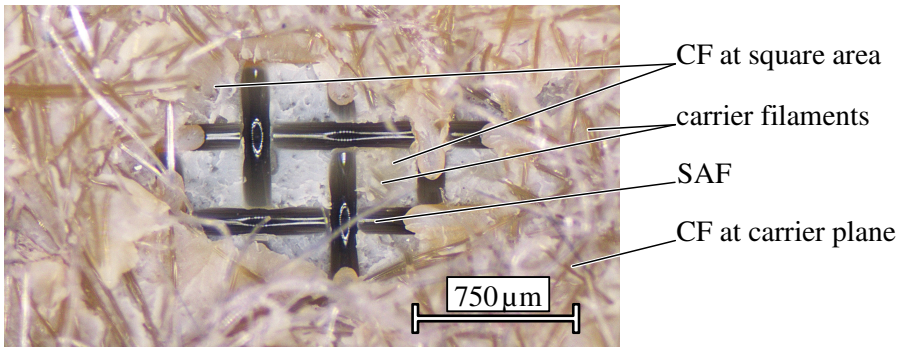


Figure 9: Special adhesion failure observed in specimen configuration *DCB D*.

The secondary bonded specimen configurations show a lower $G_{IC}$ value in wet condition than in dry condition. This reduction in $G_{IC}$ value is clearly not an effect of a change in failure mode proportions, as demonstrated by configuration *DCB C*, where both sets of specimens have very similar

portions of failure modes. The reason why the secondary bonded specimens do not show the same increase in fracture toughness by moisturisation as the co-bonded specimens must be linked to the different failure modes occurring in the two test series. The co-bonded specimens failed mainly in the repair prepreg *CFRP B*, while the secondary bonded specimens failed mainly inside *adhesive A*. The reason for the opposite behavior could be that the matrix material of the repair prepreg is a rather unmodified epoxy, while *adhesive A* is a highly modified epoxy [9].

*DCB D* shows the highest overall $G_{IC}$ values in dry and in wet condition, even though the failure mode is comprised of some substrate failure and some special adhesion failure. In order to investigate this phenomenon, configuration *DCB E* was produced. The *DCB E* specimens were produced with a clean but untreated polyester SMF with a relatively low porosity that led to a cohesively fractured surface area $\bar{A}_c$ of only 40 %. The large portion of fibre imprint areas led to a higher amount of special adhesion failure. However, no significant drop in fracture toughness could be witnessed. It seems that this new type of failure does not significantly affect the quality of a bonded joint and that the heterogeneity of the bond might even result in crack stopping capabilities. The conclusion drawn from this result is not a recommendation to use polyester fabrics in our method, but rather that bonding on surfaces produced by peeling the presented fabrics is remarkably robust.

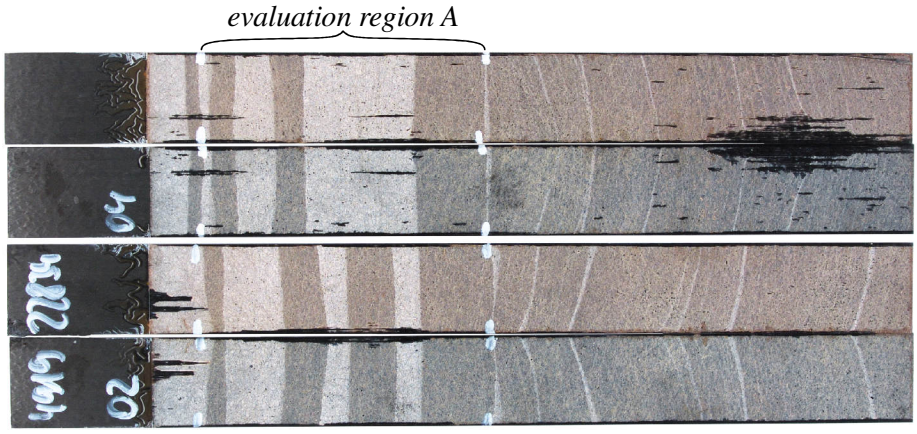


Figure 10: The fracture surface of two tested specimens of configuration *DCB C*.

## 5 CONCLUSIONS

Advances in the novel method for the certification of adhesively bonded composite repairs are presented that underline the functional principle and the practical feasibility of the method. An improved coupon for lab testing of adhesive bonds was developed that features optimised manufacturability and that enables better visual detectability of bonding defects. A case is presented on the capability of the adhesion test to detect bonding defects. The case shows that the visual detection threshold for bonding defects is very low and that even very small defects can be identified visually without the aid of technical devices. It is also shown that bondline defects can be readily identified with the aid of the peeling diagram. The detectability was found to depend on the size and orientation of the defect, as well as the relative deviation from the nominal peeling resistance of the adhesive. It is pointed out that the detection of bonding defects via the peeling diagram can be greatly adjusted by the width of the peel specimen.

A test series is presented that shows that the adhesion test can be performed on a stepped CFRP surface made of unidirectional tape material. The peel test was conducted with two different types of fabrics and with a peeling direction alongside, down and up the steps. No substrate failure occurred in the test series despite the stepped surface and the quasi-isotropic layup, showing the ability to successfully perform the adhesion test even on complex surface geometries found in repair scenarios.

The bondability of the tested layer of adhesive is investigated in two different test series by means of the DCB test. The tests were performed at room temperature with dry and with moisturised specimens. In the first test series, co-bonded specimens were produced with unidirectional carbon fibre repair prepreg. The specimens prepared according to our new method were made by laminating the repair prepreg directly onto a layer of adhesive that was tested with a steel fabric. The test results show

that the interface between the prepreg matrix and the tested adhesive features excellent quality, since no adhesion failure occurred in both dry and wet condition.
In the second test series, secondary bonded specimens were produced. The specimens prepared according to our new method were made by bonding a second CFRP panel onto the tested layer of adhesive via another adhesive film. The first layer of adhesive was tested by peeling different fabrics made of steel and polyester. The results of the second test series show that the interface between the second layer of adhesive and the tested layer of adhesive is of excellent quality if a steel fabric is used. The specimens prepared with polyester fabrics exhibit some adhesion failure at the fibre imprints even if medical grade cleaned fabrics are used. However, the tests performed with the polyester fabrics also show that the special adhesion failure occurring only at the fibre imprints leads to no significant drop in mode I fracture toughness.

In conclusion, the presented advances in the development of our method show that the adhesion test can be realised with porous fabrics, that the adhesion test is capable of detecting bonding defects and that the test can be applied on complex surfaces that are characteristic for repair scenarios. The tested layer of adhesive produced with steel fabrics exhibits excellent bonding properties that allow the formation of an adhesive bond towards a repair patch with very high process reliability and robustness. It can therefore be assumed that a successful implementation of the method in practice is possible.

In our upcoming articles, we will present test results that highlight the performance of our peel coupon as an inexpensive and powerful alternative to the DCB test for the characterisation of surface pre-treatment processes and adhesive bonds. Furthermore, we will present a case how the investigated fabrics can be used as a peel ply for structural bonding (patent pending) that enables cost-efficient, rapid and reliable surface pre-treatment in the production of FRPs.

## REFERENCES


[1] L. Heilmann, P. Wierach and M. Wiedemann, Proofed bonding – a novel method for verifying adhesion in adhesively bonded composite repairs, *Proceedings of ECCM 18 – 18th European Conference on Composite Materials, Athens, Greece, 24-28th June 2018.*

[2] U.P. Breuer, *Commercial Aircraft Composite Technology*, Springer International, 2016.

[3] C.H. Wang and C.N. Duong, *Bonded joints and repairs to composite airframe structures*, Elsevier, 2016.

[4] U.S. Department of Transportation – Federal Aviation Administration, *Policy Statement PS-AIR-100-14-130-001. Subject: Bonded Repair Size Limits.* AIR-100, 24.11.2014.

[5] U.S. Department of Transportation – Federal Aviation Administration, *Advisory Circular AC 20-107B. Subject: Composite Aircraft Structure.* AIR-100, 08.09.2009.

[6] European Aviation Safety Agency, *Acceptable Means of Compliance AMC 20-29, Composite Aircraft Structure.* Annex II to ED Decision 2010/003/R of 19.07.2010.

[7] European Standard EN 2243-2, *Aerospace series – Non-metallic materials – Structural adhesives – Test method – Part 2: Peel metal-metal*, Beuth Verlag Berlin, October 2005.

[8] European Standard DIN EN 2823, *Aerospace series – Fibre reinforced plastics – Determination of the effect of exposure to humid atmosphere on physical and mechanical characteristics*, Beuth Verlag Berlin, March 2017.

[9] R. Selzer and K. Friedrich, Mechanical properties and failure behaviour of carbon fibre-reinforced polymer composites under the influence of moisture, *Composites Part A,* **28**A, 1997, pp. 595-604.

[10] L.J. Hart-Smith, G. Redmond and M.J. Davis, The Curse of the Nylon Peel Ply, *41st International SAMPE Symposium and Exhibition*, March 25-28, 1996.

[11] M.v. Hayek-Boelingen, *Wege zum kontaminationstoleranten Kleben*, dissertation, Bundeswehr University Munich, 2004.

[12] J.v. Czarnecki, M.v. Hayek-Boelingen, H.-J. Gudladt, H. Schenkel, Kontaminationstolerantes Kleben – aktueller Stand der Entwicklung, *Adhäsion Kleben & Dichten*, **4**, 2004.